Composite Structures 92 (2010) 1744–1752

Contents lists available at ScienceDirect

Composite Structures

journal homepage: www.elsevier.com/locate/compstruct

Thermal buckling analysis of moderately thick functionally graded annular sector plates

A.R. Saidi *, A. Hasani Baferani

Department of Mechanical Engineering, Shahid Bahonar University of Kerman, Kerman, Iran

ARTICLE INFO

Article history:
Available online 11 January 2010

Keywords:
Thermal buckling
Functionally graded
Annular sector plate
First order shear deformation theory
Analytical method

ABSTRACT

In this article, thermal buckling analysis of moderately thick functionally graded annular sector plate is studied. The equilibrium and stability equations are derived using first order shear deformation plate theory. These equations are five highly coupled partial differential equations. By using an analytical method, the coupled stability equations are replaced by four decoupled equations. Solving the decoupled equations and satisfying the boundary conditions, the critical buckling temperature is found analytically. To this end, it is assumed that the annular sector plate is simply supported in radial edges and it has arbitrary boundary conditions along the circular edges. Thermal buckling of functionally graded annular sector plate for two types of thermal loading, uniform temperature rise and gradient through the thickness, are investigated. Finally, the effects of boundary conditions, power law index, plate thickness, annularity and sector angle on the critical buckling temperature of functionally graded annular sector plates are discussed in details.

1. Introduction

Functionally graded materials (FGM's) have gained much attention as advanced structural materials in recent years because of their heat resistance properties. The concept of functionally graded material was proposed in 1984 by the material scientists in the Sendai area of Japan [1–3]. FGM's are microscopically inhomogeneous in which their mechanical and thermal properties vary smoothly and continuously from one surface to the other. This is achieved by gradually varying the volume fraction of the material constituents. Typically, these materials are made from a mixture of ceramics and metal. The ceramic part of functionally graded (FG) plate provides the high temperature resistance due to its low thermal conductivity and its metal constituent resists the failure of the plate. FGM's are high performances heat resistant which are materials able to withstand ultra high temperature and extremely large thermal gradients used in aerospace industries. Designs of airframes for high speed flight and spacecraft structures have to consider carefully the effect of the thermal environment on structural and material behavior. The FG plates are used as thermal barriers in aerospace missiles in which the ceramic face of the plate is exposed to high temperature. The annular sector plates have different applications especially for space vehicles, defense industries, chemical plants, semiconductors and biomedical sectors [4].

Bending, buckling and thermal buckling of FG structural components have been extensively studied in the literatures. Javaheri and Eslami [5,6] presented the thermal buckling analysis of functionally graded simply supported rectangular plates based on classical and third order shear deformation plate theories. They obtained closed form solutions for four types of thermal loads. Najafizadeh and Eslami [7] investigated closed form solutions for thermoelastic stability of orthotropic circular plates based on classical plate theory. They also studied the thermoelastic stability of simply supported and clamped FG circular plates based on first order shear deformation plate theory [8]. Najafizadeh and Heydari [9] studied the thermal buckling of functionally graded circular plates based on higher order shear deformation plate theory and presented a closed form solution for clamped circular plates. Lanhe [10] performed closed form solution for the thermal buckling analysis of a simply supported moderately thick rectangular FG plate based on first order shear deformation plate theory. Yang et al. [11] studied second-order statistics of the elastic buckling of functionally graded rectangular plates. Ganapathi and Prakash [12] investigated thermal buckling analysis of simply supported functionally graded skew plates. They used the first order shear deformation theory in conjunction with the finite element approach. Morimoto et al. [13] studied the thermal buckling of functionally graded rectangular plates subjected to partial heating. Abrate [14] showed that the natural frequencies of FG plates are proportional to those of homogeneous isotropic plates. He also obtained the same results for buckling loads and static deflection of FG plates. Shariat and Eslami [15] presented a closed form solution for thermal buckling of

* Corresponding author. Tel.: +98 341 2111763; fax: +98 341 2120964.
E-mail address: saidi@mail.uk.ac.ir (A.R. Saidi).

0263-8223/$ - see front matter © 2010 Elsevier Ltd. All rights reserved.
doi:10.1016/j.compstruct.2010.01.004

imperfect FG rectangular plates based on classical plate theory. Also, they [16] studied buckling of thick functionally graded plates under mechanical and thermal loads based on third order shear deformation plate theory and obtained closed form solution for each loading case.

Saidi et al. [17] performed the axisymmetric bending and buckling analysis of thick functionally graded circular plates based on unconstrained third order shear deformation plate theory. Using fourth order shear deformation theory, Sahraee and Saidi [18] presented a closed form solution for axisymmetric bending of functionally graded circular plates under clamped boundary conditions. Jomehzadeh et al. [19] investigated the stress analysis of functionally graded annular sector plates based on first order shear deformation theory for different boundary conditions. They found the bending–stretching equilibrium equations and solved them to find the stresses and deflection of the FG annular sector plates under transverse mechanical loads. Zhao et al. [20] studied the mechanical and thermal buckling analysis of functionally graded rectangular plates using the first order shear deformation theory. They employed the formulation by conjunction with the element-free *KP-Ritz* method. Matsunaga [21] performed thermal buckling of functionally graded rectangular plates according to a 2D higher-order deformation theory.

To the best of author's knowledge, the subject of thermal buckling of functionally graded annular sector plates has not been performed in a specified work, yet.

In this work, an analytical solution for thermal buckling of functionally graded annular sector plates based on first order shear deformation plate theory is presented. Five coupled stability equations of FG annular sector plates are converted to four decoupled equations in terms of displacement components and a new function. Solving the decoupled equations and satisfying the boundary conditions yields the critical buckling temperature for FG annular sector plate. Finally, the effect of boundary conditions, power law index, plate thickness, sector angle and annularity on critical buckling temperature of FG annular sector plates for two types of thermal loading are discussed in detail.

2. Fundamental equations for functionally graded annular sector plates

Consider a FG annular sector plate with inner radius a, outer radius b, uniform thickness h and sector angle β (Fig. 1). It is assumed that the overall material properties of the FG plate vary through the thickness coordinate $z(-h/2 \leqslant z \leqslant h/2)$ as follow:

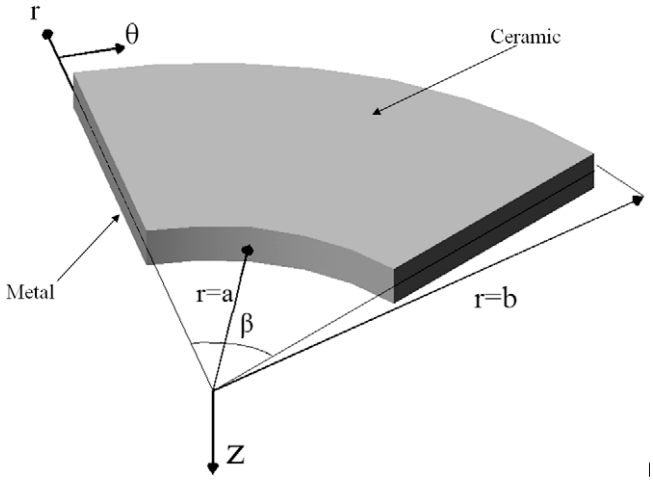

Fig. 1. Geometry and coordinate system of an annular sector plate.

$$P(z) = P_m + (P_c - P_m)\left(\frac{1}{2} - \frac{z}{h}\right)^n \tag{1}$$

where $P(z)$ denotes a material property of FG plate which may be substituted with modulus of elasticity, $E(z)$, the coefficient of thermal expansion, $\alpha(z)$, or the coefficient of thermal conductivity, $K(z)$. The subscripts m and c refer to the metal and ceramic constituents, respectively. Also n is the power law index which takes values greater than or equal to zero. Due to small changes of the Poisson ratio ν, it is assumed to be a constant through the thickness (see e.g. Refs. [5–10,17,18]).

Based on the first order shear deformation plate theory, the displacement components of the plate in r, θ and z directions are assumed to be [25]

$$\begin{aligned} u_r(r,\theta,z) &= u(r,\theta) + z\psi_r(r,\theta) \\ u_\theta(r,\theta,z) &= v(r,\theta) + z\psi_\theta(r,\theta) \\ u_z(r,\theta,z) &= w(r,\theta) \end{aligned} \tag{2}$$

where u, v and w are the displacements components in r, θ and z directions, respectively and ψ_r, ψ_θ are the rotation functions of the middle surface. The nonlinear strain–displacement components are defined as [25]

$$\begin{aligned} \varepsilon_{rr} &= \frac{\partial u}{\partial r} + \frac{1}{2}\left(\frac{\partial w}{\partial r}\right)^2 + z\frac{\partial \psi_r}{\partial r} \\ \varepsilon_{\theta\theta} &= \frac{1}{r}\left(u + \frac{\partial v}{\partial \theta}\right) + \frac{1}{2r^2}\left(\frac{\partial w}{\partial \theta}\right)^2 + \frac{z}{r}\left(\psi_r + \frac{\partial \psi_\theta}{\partial \theta}\right) \\ 2\varepsilon_{r\theta} &= \frac{1}{r}\frac{\partial u}{\partial \theta} + \frac{\partial v}{\partial r} - \frac{v}{r} + \frac{1}{r}\left(\frac{\partial w}{\partial r}\right)\left(\frac{\partial w}{\partial \theta}\right) + z\left(\frac{1}{r}\frac{\partial \psi_r}{\partial \theta} + \frac{\partial \psi_\theta}{\partial r} - \frac{\psi_\theta}{r}\right) \\ 2\varepsilon_{rz} &= \frac{\partial w}{\partial r} + \psi_r \\ 2\varepsilon_{\theta z} &= \frac{1}{r}\frac{\partial w}{\partial \theta} + \psi_\theta \end{aligned} \tag{3}$$

where ε_{rr} and $\varepsilon_{\theta\theta}$ are the normal strain components and $\varepsilon_{r\theta}, \varepsilon_{\theta z}$ and ε_{rz} are the shear strains. Considering the thermal effects, the Hooke's law for a FG annular sector plates requires [25]

$$\begin{aligned} \sigma_{rr} &= \frac{E(z)}{1-\nu^2}(\varepsilon_{rr} + \nu\varepsilon_{\theta\theta} - (1+\nu)\alpha(z)T(r,\theta,z)) \\ \sigma_{\theta\theta} &= \frac{E(z)}{1-\nu^2}(\varepsilon_{\theta\theta} + \nu\varepsilon_{rr} - (1+\nu)\alpha(z)T(r,\theta,z)) \\ \sigma_{r\theta} &= \frac{E(z)}{2(1+\nu)}(2\varepsilon_{r\theta}) \\ \sigma_{\theta z} &= \frac{E(z)}{2(1+\nu)}(2\varepsilon_{\theta z}) \\ \sigma_{rz} &= \frac{E(z)}{2(1+\nu)}(2\varepsilon_{rz}) \end{aligned} \tag{4}$$

where $\sigma_{rr}, \sigma_{\theta\theta}$ and $\sigma_{r\theta}, \sigma_{\theta z}, \sigma_{rz}$ are the normal and shear stress components, respectively. By using the principle of minimum total potential energy for a FG annular sector plate, the equilibrium equations can be obtained as [22,23]

$$\begin{aligned} &\frac{\partial N_{rr}}{\partial r} + \frac{1}{r}\frac{\partial N_{r\theta}}{\partial \theta} + \frac{N_{rr} - N_{\theta\theta}}{r} = 0 \\ &\frac{\partial N_{r\theta}}{\partial r} + \frac{1}{r}\frac{\partial N_{\theta\theta}}{\partial \theta} + \frac{2N_{r\theta}}{r} = 0 \\ &\frac{\partial M_{rr}}{\partial r} + \frac{1}{r}\frac{\partial M_{r\theta}}{\partial \theta} + \frac{M_{rr} - M_{\theta\theta}}{r} - Q_r = 0 \\ &\frac{\partial M_{r\theta}}{\partial r} + \frac{1}{r}\frac{\partial M_{\theta\theta}}{\partial \theta} + \frac{2M_{r\theta}}{r} - Q_\theta = 0 \\ &\frac{\partial Q_r}{\partial r} + \frac{1}{r}\frac{\partial Q_\theta}{\partial \theta} + \frac{Q_r}{r} + \frac{1}{r}\frac{\partial}{\partial r}\left(rN_{rr}\frac{\partial w}{\partial r}\right) + \frac{1}{r^2}\frac{\partial}{\partial \theta}\left(N_{\theta\theta}\frac{\partial w}{\partial \theta}\right) = 0 \end{aligned} \tag{5}$$

where $N_{rr}, N_{\theta\theta}$ and $N_{r\theta}$ are the in-plane resultant forces, $M_{rr}, M_{\theta\theta}$ and $M_{r\theta}$ are the bending and twisting moment intensities and Q_r and Q_θ are the out of plane resultant forces. These parameters are defined as

$$\begin{aligned}(N_{rr}, N_{\theta\theta}, N_{r\theta}) &= \int_{-h/2}^{h/2} (\sigma_{rr}, \sigma_{\theta\theta}, \sigma_{r\theta}) dz \\ (M_{rr}, M_{\theta\theta}, M_{r\theta}) &= \int_{-h/2}^{h/2} (\sigma_{rr}, \sigma_{\theta\theta}, \sigma_{r\theta}) z dz \\ (Q_r, Q_\theta) &= k^2 \int_{-h/2}^{h/2} (\sigma_{rz}, \sigma_{\theta z}) dz\end{aligned} \tag{6}$$

In the third equation of (6), k^2 is the shear correction factor, which is assumed to be 5/6. Substituting Eqs. (1), (3) and (4) into Eq. (6) gives us the following relations for resultant forces and moments

$$\begin{aligned}
N_{rr} &= A_{11}\frac{\partial u}{\partial r} + A_{12}\left(\frac{u}{r} + \frac{1}{r}\frac{\partial v}{\partial \theta}\right) + B_{11}\frac{\partial \psi_r}{\partial r} + B_{12}\left(\frac{\psi_r}{r} + \frac{1}{r}\frac{\partial \psi_\theta}{\partial \theta}\right) - \frac{T_N}{1-v} \\
N_{\theta\theta} &= A_{11}\left(\frac{u}{r} + \frac{1}{r}\frac{\partial v}{\partial \theta}\right) + A_{12}\frac{\partial u}{\partial r} + B_{11}\left(\frac{\psi_r}{r} + \frac{1}{r}\frac{\partial \psi_\theta}{\partial \theta}\right) + B_{12}\frac{\partial \psi_r}{\partial r} - \frac{T_N}{1-v} \\
N_{r\theta} &= A_{33}\left(\frac{1}{r}\frac{\partial v}{\partial \theta} + \frac{\partial u}{\partial r} - \frac{u}{r}\right) + B_{33}\left(\frac{1}{r}\frac{\partial \psi_r}{\partial \theta} + \frac{\partial \psi_\theta}{\partial r} - \frac{\psi_\theta}{r}\right) \\
M_{rr} &= B_{11}\frac{\partial u}{\partial r} + B_{12}\left(\frac{u}{r} + \frac{1}{r}\frac{\partial v}{\partial \theta}\right) + D_{11}\frac{\partial \psi_r}{\partial r} + D_{12}\left(\frac{\psi_r}{r} + \frac{1}{r}\frac{\partial \psi_\theta}{\partial \theta}\right) - \frac{T_M}{1-v} \\
M_{\theta\theta} &= B_{11}\left(\frac{u}{r} + \frac{1}{r}\frac{\partial v}{\partial \theta}\right) + B_{12}\frac{\partial u}{\partial r} + D_{11}\left(\frac{\psi_r}{r} + \frac{1}{r}\frac{\partial \psi_\theta}{\partial \theta}\right) + D_{12}\frac{\partial \psi_r}{\partial r} - \frac{T_M}{1-v} \\
M_{r\theta} &= B_{33}\left(\frac{1}{r}\frac{\partial v}{\partial \theta} + \frac{\partial u}{\partial r} - \frac{u}{r}\right) + D_{33}\left(\frac{1}{r}\frac{\partial \psi_r}{\partial \theta} + \frac{\partial \psi_\theta}{\partial r} - \frac{\psi_\theta}{r}\right) \\
Q_r &= k^2 A_{33}\left(\frac{\partial w}{\partial r} + \psi_r\right) \\
Q_\theta &= k^2 A_{33}\left(\frac{1}{r}\frac{\partial w}{\partial \theta} + \psi_\theta\right)
\end{aligned} \tag{7}$$

where $A_{11}, B_{11}, D_{11}, \ldots$ are the material stiffness coefficients of the plate which can be defined in the form

$$\begin{aligned}(A_{11}, B_{11}, D_{11}) &= \int_{-h/2}^{h/2} \frac{E(z)}{1-v^2}(1, z, z^2) dz \\ (A_{12}, B_{12}, D_{12}) &= \int_{-h/2}^{h/2} \frac{vE(z)}{1-v^2}(1, z, z^2) dz \\ (A_{33}, B_{33}, D_{33}) &= \int_{-h/2}^{h/2} \frac{E(z)}{2(1+v)}(1, z, z^2) dz\end{aligned} \tag{8}$$

Also, the thermal terms T_N and T_M are defined as

$$\begin{aligned}T_N &= \int_{-h/2}^{h/2} E(z)\alpha(z)T(r, \theta, z) dz \\ T_M &= \int_{-h/2}^{h/2} E(z)\alpha(z)T(r, \theta, z) z\, dz\end{aligned} \tag{9}$$

3. Stability equations

In this section, the stability equations of the FG plate are derived by using the adjacent equilibrium criterion [24]. It is assumed that the plate is in the equilibrium configuration (u^0, v^0, w^0) whose stability is under investigation. The displacement components of a neighboring configuration of the stable state can be expressed as follows:

$$\begin{aligned}u &= u^0 + u^1 \\ v &= v^0 + v^1 \\ w &= w^0 + w^1 \\ \psi_r &= \psi_r^0 + \psi_r^1 \\ \psi_\theta &= \psi_\theta^0 + \psi_\theta^1\end{aligned} \tag{10}$$

where u^1, v^1 and w^1 are the infinitesimal increments from the stable configuration. Similarly, the resultant forces of a neighboring state can be expressed as

$$\begin{aligned}
N_{rr} &= N_{rr}^0 + N_{rr}^1 \\
N_{\theta\theta} &= N_{\theta\theta}^0 + N_{\theta\theta}^1 \\
N_{r\theta} &= N_{r\theta}^0 + N_{r\theta}^1 \\
M_{rr} &= M_{rr}^0 + M_{rr}^1 \\
M_{\theta\theta} &= M_{\theta\theta}^0 + M_{\theta\theta}^1 \\
M_{r\theta} &= M_{r\theta}^0 + M_{r\theta}^1 \\
Q_{rr} &= Q_{rr}^0 + Q_{rr}^1 \\
Q_{\theta\theta} &= Q_{\theta\theta}^0 + Q_{\theta\theta}^1
\end{aligned} \tag{11}$$

where $N_{rr}^0, N_{\theta\theta}^0$ and $N_{r\theta}^0$ corresponding to u^0, v^0 and w^0, and $N_{rr}^1, N_{\theta\theta}^1$ and $N_{r\theta}^1$ are the variations in the in-plane resultants corresponding to u^1, v^1 and w^1. The stability equations can be obtained by substituting Eqs. (10) and (11) into Eq. (5). Upon substitution, the terms in the consequent equations with subscript 0 satisfy the equilibrium conditions and therefore drop out of the equations. Also the nonlinear terms with subscript 1 are ignored because they are small with the linear terms. The remaining terms from the stability equations of an annular sector plate under thermal loads yields the following partial differential equations

$$\begin{aligned}
&\frac{\partial N_{rr}^1}{\partial r} + \frac{1}{r}\frac{\partial N_{r\theta}^1}{\partial \theta} + \frac{N_{rr}^1 - N_{\theta\theta}^1}{r} = 0 \\
&\frac{\partial N_{r\theta}^1}{\partial r} + \frac{1}{r}\frac{\partial N_{\theta\theta}^1}{\partial \theta} + \frac{2N_{r\theta}^1}{r} = 0 \\
&\frac{\partial M_{rr}^1}{\partial r} + \frac{1}{r}\frac{\partial M_{r\theta}^1}{\partial \theta} + \frac{M_{rr}^1 - M_{\theta\theta}^1}{r} - Q_{rr}^1 = 0 \\
&\frac{\partial M_{r\theta}^1}{\partial r} + \frac{1}{r}\frac{\partial M_{\theta\theta}^1}{\partial \theta} + \frac{2M_{r\theta}^1}{r} - Q_{\theta\theta}^1 = 0
\end{aligned} \tag{12}$$

$$\frac{\partial Q_{rr}^1}{\partial r} + \frac{1}{r}\frac{\partial Q_{\theta\theta}^1}{\partial \theta} + \frac{Q_{rr}^1}{r} + \frac{1}{r}\frac{\partial}{\partial r}\left(rN_{rr}^0\frac{\partial w^1}{\partial r}\right) + \frac{1}{r^2}\frac{\partial}{\partial \theta}\left(N_{\theta\theta}^0\frac{\partial w^1}{\partial \theta}\right) = 0$$

Substituting the resultant forces and moments from Eq. (7) into Eq. (12), the stability equations are obtained as

$$\begin{aligned}
&A_{11}\left(\frac{\partial^2 u^1}{\partial r^2} + \frac{1}{r}\frac{\partial u^1}{\partial r} - \frac{u^1}{r^2} - \frac{1}{r^2}\frac{\partial v^1}{\partial \theta} + \frac{1}{r}\frac{\partial^2 v^1}{\partial r \partial \theta}\right) \\
&+ A_{33}\left(\frac{1}{r^2}\frac{\partial^2 u^1}{\partial \theta^2} - \frac{1}{r}\frac{\partial^2 v^1}{\partial r \partial \theta} - \frac{1}{r^2}\frac{\partial v^1}{\partial \theta}\right) \\
&+ B_{11}\left(\frac{\partial^2 \psi_r^1}{\partial r^2} + \frac{1}{r}\frac{\partial \psi_r^1}{\partial r} - \frac{\psi_r^1}{r^2} - \frac{1}{r^2}\frac{\partial \psi_\theta^1}{\partial \theta} + \frac{1}{r}\frac{\partial^2 \psi_\theta^1}{\partial r \partial \theta}\right) \\
&+ B_{33}\left(\frac{1}{r^2}\frac{\partial^2 \psi_r^1}{\partial \theta^2} - \frac{1}{r}\frac{\partial^2 \psi_\theta^1}{\partial r \partial \theta} - \frac{1}{r^2}\frac{\partial \psi_\theta^1}{\partial \theta}\right) = 0
\end{aligned} \tag{13a}$$

$$\begin{aligned}
&A_{11}\left(\frac{1}{r^2}\frac{\partial u^1}{\partial \theta} + \frac{1}{r}\frac{\partial^2 u^1}{\partial r \partial \theta} + \frac{1}{r^2}\frac{\partial^2 v^1}{\partial \theta^2}\right) \\
&+ A_{33}\left(\frac{-1}{r}\frac{\partial^2 u^1}{\partial r \partial \theta} + \frac{\partial^2 v^1}{\partial r^2} + \frac{1}{r^2}\frac{\partial u^1}{\partial \theta} + \frac{1}{r}\frac{\partial v^1}{\partial r} - \frac{v^1}{r^2}\right) \\
&+ B_{11}\left(\frac{1}{r}\frac{\partial \psi_r^1}{\partial \theta} + \frac{1}{r^2}\frac{\partial^2 \psi_\theta^1}{\partial \theta^2} + \frac{1}{r}\frac{\partial^2 \psi_r^1}{\partial r \partial \theta}\right) \\
&+ B_{33}\left(\frac{-1}{r}\frac{\partial^2 \psi_r^1}{\partial r \partial \theta} + \frac{\partial^2 \psi_\theta^1}{\partial r^2} + \frac{1}{r^2}\frac{\partial \psi_\theta^1}{\partial \theta} + \frac{1}{r}\frac{\partial \psi_\theta^1}{\partial r} - \frac{\psi_\theta^1}{r^2}\right) = 0
\end{aligned} \tag{13b}$$

$$B_{11}\left(\frac{\partial^2 u^1}{\partial r^2}+\frac{1}{r}\frac{\partial u^1}{\partial r}-\frac{u^1}{r^2}-\frac{1}{r^2}\frac{\partial v^1}{\partial \theta}+\frac{1}{r}\frac{\partial^2 v^1}{\partial r\partial\theta}\right)+B_{33}\left(\frac{1}{r^2}\frac{\partial^2 u^1}{\partial\theta^2}-\frac{1}{r}\frac{\partial^2 v^1}{\partial r\partial\theta}-\frac{1}{r^2}\frac{\partial v^1}{\partial\theta}\right)+D_{11}\left(\frac{\partial^2\psi_r^1}{\partial r^2}+\frac{1}{r}\frac{\partial\psi_r^1}{\partial r}-\frac{\psi_r^1}{r^2}-\frac{1}{r^2}\frac{\partial\psi_\theta^1}{\partial\theta}+\frac{1}{r}\frac{\partial^2\psi_\theta^1}{\partial r\partial\theta}\right)+D_{33}\left(\frac{1}{r^2}\frac{\partial^2\psi_r^1}{\partial\theta^2}-\frac{1}{r}\frac{\partial^2\psi_\theta^1}{\partial r\partial\theta}-\frac{1}{r^2}\frac{\partial\psi_\theta^1}{\partial\theta}\right)-k^2A_{33}\left(\frac{\partial w^1}{\partial r}+\psi_r^1\right)=0 \tag{13c}$$

$$B_{11}\left(\frac{1}{r^2}\frac{\partial u^1}{\partial\theta}+\frac{1}{r}\frac{\partial^2 u^1}{\partial r\partial\theta}+\frac{1}{r^2}\frac{\partial^2 v^1}{\partial\theta^2}\right)+B_{33}\left(\frac{-1}{r}\frac{\partial^2 u^1}{\partial r\partial\theta}+\frac{\partial^2 v^1}{\partial r^2}+\frac{1}{r^2}\frac{\partial u^1}{\partial\theta}+\frac{1}{r}\frac{\partial v^1}{\partial r}-\frac{v^1}{r^2}\right)+D_{11}\left(\frac{1}{r}\frac{\partial\psi_r^1}{\partial\theta}+\frac{1}{r^2}\frac{\partial^2\psi_\theta^1}{\partial\theta^2}+\frac{1}{r}\frac{\partial^2\psi_r^1}{\partial r\partial\theta}\right)+D_{33}\left(\frac{-1}{r}\frac{\partial^2\psi_r^1}{\partial r\partial\theta}+\frac{\partial^2\psi_\theta^1}{\partial r^2}+\frac{1}{r^2}\frac{\partial\psi_\theta^1}{\partial\theta}+\frac{1}{r}\frac{\partial\psi_\theta^1}{\partial r}-\frac{\psi_\theta^1}{r^2}\right)-k^2A_{33}\left(\frac{1}{r}\frac{\partial w^1}{\partial\theta}+\psi_\theta^1\right)=0 \tag{13d}$$

$$k^2A_{33}\left(\frac{\partial^2 w^1}{\partial r^2}+\frac{1}{r}\frac{\partial w^1}{\partial r}+\frac{1}{r^2}\frac{\partial^2 w^1}{\partial\theta^2}+\frac{\partial\psi_r^1}{\partial r}+\frac{1}{r}\frac{\partial\psi_\theta^1}{\partial\theta}+\frac{\psi_r^1}{r}\right)+\frac{1}{r}\frac{\partial}{\partial r}\left(rN_{rr}^0\frac{\partial w^1}{\partial r}\right)+\frac{1}{r^2}\frac{\partial}{\partial\theta}\left(N_{\theta\theta}^0\frac{\partial w^1}{\partial\theta}\right)=0 \tag{13e}$$

Eq. (13) are five highly coupled partial differential equations in terms of in-plane displacements, rotation functions and transverse displacement. These equations can not be solved easily. For solving these equations analytically, it is desirable to find a method for decoupling them. Using the following analytical method, these stability equations will be decoupled.

Eq. (13) can be easily rewritten in the form

$$A_{11}\frac{\partial\varphi_1}{\partial r}+A_{33}\frac{1}{r}\frac{\partial\varphi_2}{\partial\theta}+B_{11}\frac{\partial\varphi_3}{\partial r}+B_{33}\frac{1}{r}\frac{\partial\varphi_4}{\partial\theta}=0 \tag{14a}$$

$$A_{11}\frac{1}{r}\frac{\partial\varphi_1}{\partial\theta}-A_{33}\frac{\partial\varphi_2}{\partial r}+B_{11}\frac{1}{r}\frac{\partial\varphi_3}{\partial\theta}-B_{33}\frac{\partial\varphi_4}{\partial r}=0 \tag{14b}$$

$$B_{11}\frac{\partial\varphi_1}{\partial r}+B_{33}\frac{1}{r}\frac{\partial\varphi_2}{\partial\theta}+D_{11}\frac{\partial\varphi_3}{\partial r}+D_{33}\frac{1}{r}\frac{\partial\varphi_4}{\partial\theta}-k^2A_{33}\left(\frac{\partial w^1}{\partial r}+\psi_r^1\right)=0 \tag{14c}$$

$$B_{11}\frac{1}{r}\frac{\partial\varphi_1}{\partial\theta}-B_{33}\frac{\partial\varphi_2}{\partial r}+D_{11}\frac{1}{r}\frac{\partial\varphi_3}{\partial\theta}-D_{33}\frac{\partial\varphi_4}{\partial r}-k^2A_{33}\left(\frac{1}{r}\frac{\partial w^1}{\partial\theta}+\psi_\theta^1\right)=0 \tag{14d}$$

$$k^2A_{33}(\nabla^2 w^1+\varphi_3)+\frac{1}{r}\frac{\partial}{\partial r}\left(rN_{rr}^0\frac{\partial w^1}{\partial r}\right)+\frac{1}{r^2}\frac{\partial}{\partial\theta}\left(N_{\theta\theta}^0\frac{\partial w^1}{\partial\theta}\right)=0 \tag{14e}$$

where ∇^2 is the Laplace operator in polar coordinates $\left(\nabla^2=\frac{\partial^2}{\partial r^2}+\frac{1}{r}\frac{\partial}{\partial r}+\frac{1}{r^2}\frac{\partial^2}{\partial\theta^2}\right)$ and the variables $\varphi_1,\varphi_2,\varphi_3$ and φ_4 are defined as

$$\begin{aligned}\varphi_1&=\frac{\partial u^1}{\partial r}+\frac{u^1}{r}+\frac{1}{r}\frac{\partial v^1}{\partial\theta}\\ \varphi_2&=\frac{1}{r}\frac{\partial u^1}{\partial\theta}-\frac{\partial v^1}{\partial r}-\frac{v^1}{r}\\ \varphi_3&=\frac{\partial\psi_r^1}{\partial r}+\frac{\psi_r^1}{r}+\frac{1}{r}\frac{\partial\psi_\theta^1}{\partial\theta}\\ \varphi_4&=\frac{1}{r}\frac{\partial\psi_r^1}{\partial\theta}-\frac{\partial\psi_\theta^1}{\partial r}-\frac{\psi_\theta^1}{r}\end{aligned} \tag{15}$$

From relations (8) it is easy to show that the material coefficients are related to each other via the relation $B_{33}=(A_{33}B_{11})/A_{11}$. Then, Eqs. (14a) and (14b) can be rewritten in the form

$$B_{11}\frac{\partial\varphi_1}{\partial r}+B_{33}\frac{1}{r}\frac{\partial\varphi_2}{\partial\theta}=-\frac{B_{11}^2}{A_{11}}\frac{\partial\varphi_3}{\partial r}-\frac{B_{33}B_{11}}{A_{11}}\frac{1}{r}\frac{\partial\varphi_4}{\partial\theta} \tag{16a}$$

$$B_{11}\frac{1}{r}\frac{\partial\varphi_1}{\partial\theta}-B_{33}\frac{\partial\varphi_2}{\partial r}=-\frac{B_{11}^2}{A_{11}}\frac{1}{r}\frac{\partial\varphi_3}{\partial\theta}+\frac{B_{33}B_{11}}{A_{11}}\frac{\partial\varphi_4}{\partial r} \tag{16b}$$

Substituting Eqs. (16a) and (16b) into Eqs. (14c) and (14d), respectively give us the following relations

$$\left(D_{11}-\frac{B_{11}^2}{A_{11}}\right)\frac{\partial\varphi_3}{\partial r}+\left(D_{33}-\frac{B_{33}B_{11}}{A_{11}}\right)\left(\frac{1}{r}\frac{\partial\varphi_4}{\partial\theta}\right)-k^2A_{33}\left(\frac{\partial w^1}{\partial r}+\psi_r^1\right)=0 \tag{17a}$$

$$\left(D_{11}-\frac{B_{11}^2}{A_{11}}\right)\left(\frac{1}{r}\frac{\partial\varphi_3}{\partial\theta}\right)-\left(D_{33}-\frac{B_{33}B_{11}}{A_{11}}\right)\frac{\partial\varphi_4}{\partial r}-k^2A_{33}\left(\frac{1}{r}\frac{\partial w^1}{\partial\theta}+\psi_\theta^1\right)=0 \tag{17b}$$

By differentiating Eqs. (17a) and (17b) with respect to r and θ, respectively and doing some algebraic calculations, the following decoupled partial differential equations are obtained

$$\widehat{D}\nabla^4 w^1+\frac{1}{r}\frac{\partial}{\partial r}\left(rN_{rr}^0\frac{\partial w^1}{\partial r}\right)+\frac{1}{r^2}\frac{\partial}{\partial\theta}\left(N_{\theta\theta}^0\frac{\partial w^1}{\partial\theta}\right)=-\frac{\widehat{D}}{k^2A_{33}}\nabla^2\left(\frac{1}{r}\frac{\partial}{\partial r}\left(rN_{rr}^0\frac{\partial w^1}{\partial r}\right)+\frac{1}{r^2}\frac{\partial}{\partial\theta}\left(N_{\theta\theta}^0\frac{\partial w^1}{\partial\theta}\right)\right) \tag{18a}$$

$$\widehat{C}\nabla^2\varphi_4-k^2A_{33}\varphi_4=0 \tag{18b}$$

where the parameters $\widehat{D}$ and $\widehat{C}$ denote the equivalent flexural rigidities of FG plate which are defined as

$$\begin{aligned}\widehat{D}&=D_{11}-\frac{B_{11}^2}{A_{11}}\\ \widehat{C}&=D_{33}-\frac{B_{11}B_{33}}{A_{11}}\end{aligned} \tag{19}$$

Substituting Eq. (1) into Eq. (8) and integration yield

$$\begin{aligned}A_{11}&=\frac{h}{1-\nu^2}\left(E_m+\frac{E_{cm}}{n+1}\right)\\ B_{11}&=-\frac{E_{cm}h^2}{1-\nu^2}\left(\frac{n}{2(n+1)(n+2)}\right)\\ D_{11}&=\frac{E_mh^3}{12(1-\nu^2)}+\frac{E_{cm}h^3(n^2+n+2)}{4(1-\nu^2)(n+1)(n+2)(n+3)}\end{aligned} \tag{20}$$

where the parameter E_{cm} is defined as $E_{cm}=E_c-E_m$. Doing some algebraic calculations on Eq. (17), it can be concluded that

$$\psi_r^1 = -\frac{\partial}{\partial r}\left(w^1 + \frac{\widehat{D}}{k^2A_{33}}\nabla^2 w^1 + \frac{\widehat{D}}{k^4A_{33}^2} \times\left(\frac{1}{r}\frac{\partial}{\partial r}\left(rN_{rr}^0\frac{\partial w^1}{\partial r}\right) + \frac{1}{r^2}\frac{\partial}{\partial\theta}\left(N_{\theta\theta}^0\frac{\partial w^1}{\partial\theta}\right)\right)\right) + \frac{\widehat{C}}{k^2A_{33}}\left(\frac{1}{r}\frac{\partial\varphi_4}{\partial\theta}\right) \tag{21a}$$

$$\psi_\theta^1 = -\frac{1}{r}\frac{\partial}{\partial\theta}\left(w^1 + \frac{\widehat{D}}{k^2A_{33}}\nabla^2 w^1 + \frac{\widehat{D}}{k^4A_{33}^2}\left(\frac{1}{r}\frac{\partial}{\partial r}\left(rN_{rr}^0\frac{\partial w^1}{\partial r}\right) + \frac{1}{r^2}\frac{\partial}{\partial\theta}\left(N_{\theta\theta}^0\frac{\partial w^1}{\partial\theta}\right)\right)\right) - \frac{\widehat{C}}{k^2A_{33}}\left(\frac{\partial\varphi_4}{\partial r}\right) \tag{21b}$$

Using Eqs. (14a) and (14b), it is easy to show that

$$\nabla^2\varphi_2 = -\frac{B_{11}}{A_{11}}\nabla^2\varphi_4 \tag{22}$$

$$\nabla^2\varphi_1 = -\frac{B_{11}}{A_{11}}\nabla^2\varphi_3 \tag{23}$$

Substituting the definition of parameters φ_i $(i = 1,\ldots,4)$ from relations (15) into Eqs. (22) and (23), the following relations can be obtained

$$u^1 = -\frac{B_{11}}{A_{11}}\psi_r^1 \qquad v^1 = -\frac{B_{11}}{A_{11}}\psi_\theta^1 \tag{24}$$

Therefore, the five coupled partial differential equations (13) have been converted to two decoupled equations (18) and two algebraic equations (24). For thermal buckling analysis of FG annular sector plate, Eqs. (18) and (24) should be solved under various boundary conditions.

4. Thermal buckling analysis of functionally graded annular sector plate

In this section, thermal buckling analysis for two types of thermal loading, uniform temperature rise and nonlinear temperature change across the thickness, are studied. The FG annular sector plate is assumed to have simply supported radial edges and arbitrary boundary conditions along the circular edges.

4.1. Thermal buckling analysis under uniform temperature rise

To find the critical buckling temperature, T_{cr}, the pre-buckling thermal stresses should be evaluated. Solving the membrane form of equilibrium equations and using the method developed by Meyers and Hyer [26], gives us the pre-buckling resultant forces as

$$N_{rr}^0 = -\frac{T_N}{1-\nu} \qquad N_{\theta\theta}^0 = -\frac{T_N}{1-\nu} \qquad N_{r\theta}^0 = 0 \tag{25}$$

Substituting Eq. (25) into Eq. (18) yield

$$\widehat{D}\left(1 - \frac{T_N}{k^2A_{33}(1-\nu)}\right)\nabla^4 w^1 + \frac{T_N}{1-\nu}\nabla^2 w^1 = 0 \qquad \widehat{C}\nabla^2\varphi_4 - k^2A_{33}\varphi_4 = 0 \tag{26}$$

Based on the Levy solution, for a plate with simply supported boundary conditions in radial edges, the transverse displacement w^1 and the function φ_4 are defined as [19]

$$w^1 = \sum_{m=1}^{\infty} w_m(r)\sin(\mu_m\theta) \qquad \varphi_4 = \sum_{m=1}^{\infty}\varphi_m(r)\cos(\mu_m\theta) \tag{27}$$

where μ_m denotes $\frac{m\pi}{\beta}$. By substituting Eq. (27) into Eq. (26), two ordinary differential equations are obtained. The solutions of these differential equations are as follows

$$w_m(r) = C_1 r^{\mu_m} + C_2 r^{-\mu_m} + C_3 J_{\mu_m}\left(\sqrt{\frac{k^2A_{33}T_N}{\widehat{D}(k^2A_{33}(1-\nu)-T_N)}}r\right) + C_4 Y_{\mu_m}\left(\sqrt{\frac{k^2A_{33}T_N}{\widehat{D}(k^2A_{33}(1-\nu)-T_N)}}r\right) \tag{28a}$$

$$\varphi_m(r) = C_5 I_{\mu_m}\left(\sqrt{\frac{k^2A_{33}}{\widehat{C}}}r\right) + C_6 K_{\mu_m}\left(\sqrt{\frac{k^2A_{33}}{\widehat{C}}}r\right) \tag{28b}$$

where J and Y are the Bessel functions. Also, I and K are the modified Bessel functions [27] and C_i $(i = 1,\ldots,6)$ are six unknown constants. By satisfying the arbitrary boundary conditions in circular edges, six algebraic equations in terms of unknown coefficients C_i are obtained. Setting the determinant of coefficients of these equations equal to zero, the critical buckling temperature for FG annular sector plates under uniform temperature rise is determined.

4.2. Thermal buckling analysis under nonlinear temperature change across the thickness

For functionally graded plates, the coefficient of thermal conduction $K(z)$ is a function of thickness coordinate. In the nonlinear temperature changes, the temperature through the thickness is governed by the one-dimensional Fourier equation of heat conduction. Based on Eq. (1), the coefficient of thermal conduction is defined as follows

$$K(z) = K_m + (K_c - K_m)\left(\frac{1}{2} - \frac{z}{h}\right)^n \tag{29}$$

The heat conduction equation and the boundary conditions across the plate thickness are

$$\frac{d}{dz}\left(K(z)\frac{dT}{dz}\right) = 0 \tag{30a}$$

$$T = T_m \text{ at } z = h/2 \qquad T = T_c \text{ at } z = -h/2 \tag{30b}$$

Substituting Eq. (29) into Eq. (30a) yields a second order differential equation in terms of temperature which can be written in term of the non dimensional variable s as

$$-\frac{d^2T}{ds^2} + \frac{nK_{cm}s^{n-1}}{K_m + K_{cm}s^n}\frac{dT}{ds} = 0 \tag{31a}$$

where

$$s = \frac{h-2z}{2h} \tag{31b}$$

The solution of differential equation (31a) can be easily obtained by using the polynomial series in the form [6]

$$T(z) = T_m + s\Delta T\frac{\sum_{k=0}^{\infty}\left(\frac{1}{nk+1}\left(\frac{-K_{cm}s^n}{K_m}\right)^k\right)}{\sum_{k=0}^{\infty}\left(\frac{1}{nk+1}\left(\frac{-K_{cm}}{K_m}\right)^k\right)} \tag{32}$$

where $\Delta T = T_c - T_m$ is the temperature difference between the ceramic-rich and metal-rich surfaces of the plate. Using the temperature distribution (32) together with Eq. (28) and doing a similar procedure as previous section, the critical buckling temperature for nonlinear temperature across the thickness is obtained. The pre-buckling resultant forces for this case are the same as the preceding case which are given by Eq. (25). Substituting $T(z)$ from Eq. (32) into Eqs. (9) and (26), the buckling temperature for a FG annular sector plate under nonlinear temperature change across the thickness is obtained.

5. Boundary conditions

For circular edges, the possible boundary conditions are simply supported, clamped and free. Simply supported boundary conditions in circular edges require

$$w_m^1 = M_{rr}^1 = \psi_\theta^1 = 0 \tag{33a}$$

where

$$M_{rr}^1 = \widehat{D}\frac{\partial \psi_r}{\partial r} + \widehat{C}\left(\frac{\psi_r}{r} + \frac{1}{r}\frac{\partial \psi_\theta}{\partial \theta}\right) \tag{33b}$$

Also, for clamped boundary conditions in circular edges, it can be written

$$w_m^1 = \psi_r^1 = \psi_\theta^1 = 0 \tag{34}$$

If the circular edges are free, it is reasonable to have

$$M_{rr}^1 = M_{r\theta}^1 = Q_r^1 + N_{rr}^0\frac{\partial w^1}{\partial r} = 0 \tag{35}$$

where Q_r and $M_{r\theta}$ are defined as follows [28]:

$$\begin{aligned} &Q_r^1 + N_{rr}^0\frac{\partial w^1}{\partial r} = k^2 A_{33}\left(\frac{\partial w^1}{\partial r} + \psi_r^1\right) - \frac{T_N}{1-\nu}\frac{\partial w^1}{\partial r} \\ &M_{r\theta}^1 = \widehat{C}\left(\frac{1}{r}\frac{\partial \psi_r^1}{\partial \theta} + \frac{\partial \psi_\theta^1}{\partial r} - \frac{\psi_r^1}{r}\right) \end{aligned} \tag{36}$$

It is assumed that the radial edges of FG annular sector plate are simply supported and the boundary conditions along the circular edges are identified according to the inner and outer radius of the plate (e.g. *SSCF* denotes a plate with simply supported radial edges, clamped inner and free outer circular edges). The nine possible boundary conditions containing *SSSS, SSCC, SSFF, SSCF, SSFC, SSCS, SSSC, SSSF* and *SSFS* have been considered for obtaining the numerical results.

6. Numerical results and discussions

For numerical calculations, a functionally graded annular sector plate composed of aluminum (as metal) and alumina (as ceramic) is considered. Young's modulus, coefficient of thermal expansion and thermal conductivity for aluminum are $E_m = 70$ GPa, $\alpha_m = 23 \times 10^{-6}\,^\circ\mathrm{C}^{-1}$, $K_m = 204$ W/m K and for alumina are $E_c = 380$ GPa, $\alpha_c = 7.4 \times 10^{-6}\,^\circ\mathrm{C}^{-1}$, $K_c = 10.4$ W/m K, respectively. Poisson's ratio of the plate is assumed to be constant through the thickness and equal to *0.3*.

Since, there is not any similar results for thermal buckling of sector plates in the literature, the results have been compared with the available results for square plates in Refs. [6,10]. For this purpose, the sector angle is considered to be very small (e.g. $\beta = \pi/240$). Also the inner and outer radius are considered to be very close to each other (e.g. $a = 0.987$ (m), $b = 1$ (m)) and the plate thickness is $h = 10^{-4}$ (m). Based on the results in Table 1

Table 1
Thermal buckling temperature for uniform temperature rise, comparison of annular sector plates and square plate.

n	Present (annular sector plate)	Ref. [6] (square plate)	Ref. [10] (square plate)
0	17.089	17.088	17.091
1	7.940	7.939	7.940
5	7.261	7.260	7.262
10	7.464	7.462	7.465

Table 2
Critical buckling temperature of simply supported; (SSSS) functionally graded annular sector plate under uniform temperature rise (U) and nonlinear temperature change across the thickness (NL) for some values of n and $b/h(\beta = 60, b/a = 3)$.

n		$b/h = 50$	$b/h = 20$	$b/h = 10$	$b/h = 5$
0	U	147.455	898.366	3297.247	9926.534
	NL	284.911	1786.733	6584.494	19843.068
0.5	U	83.589	510.670	1890.898	5834.841
	NL	207.293	1333.786	4974.359	15377.143
1	U	68.557	419.345	1558.889	4865.115
	NL	165.460	1078.674	4045.270	12652.433
2	U	60.776	371.652	1380.365	4296.961
	NL	134.661	885.206	3320.541	10362.068
5	U	62.648	381.419	1396.871	4180.369
	NL	124.099	810.323	2996.299	8988.369
20	U	61.603	373.571	1351.128	3910.857
	NL	113.679	740.220	2703.494	7844.322

Table 3
Critical buckling temperature of clamped; (SSCC) functionally graded annular sector plate under uniform temperature rise (U) and nonlinear temperature change across the thickness (NL) for some values of n and $b/h(\beta = 60, b/a = 3)$.

n		$b/h = 50$	$b/h = 20$	$b/h = 10$	$b/h = 5$
0	U	284.894	1672.105	5546.823	13632.376
	NL	559.789	3334.210	11083.647	27254.752
0.5	U	161.637	954.844	3221.010	8169.818
	NL	413.157	2505.368	8482.745	21536.022
1	U	132.620	785.695	2670.752	6875.786
	NL	332.234	2032.398	6939.807	17886.853
2	U	117.558	696.014	2361.832	6059.909
	NL	271.749	1668.314	5690.093	14618.348
5	U	121.015	709.128	2342.816	5715.268
	NL	249.746	1515.785	5032.647	12292.566
20	U	118.851	690.069	2228.160	5220.301
	NL	228.652	1375.858	4464.881	10474.142

Table 4
Thermal buckling temperature of free; (SSFF) functionally graded annular sector plate under uniform temperature rise (U) and nonlinear temperature change across the thickness (NL) for some values of n and $b/h(\beta = 60, b/a = 3)$.

n		$b/h = 50$	$b/h = 20$	$b/h = 10$	$b/h = 5$
0	U	25.088	154.358	596.634	2171.203
	NL	40.176	298.716	1183.268	4332.406
0.5	U	14.221	87.598	339.508	1245.207
	NL	24.324	217.867	882.320	3271.245
1	U	11.664	71.881	278.935	1026.672
	NL	17.349	174.114	713.140	2659.739
2	U	10.340	63.716	247.182	909.074
	NL	12.893	141.758	584.699	2182.703
5	U	10.659	65.563	253.251	919.841
	NL	12.183	130.375	534.414	1969.391
20	U	10.482	64.374	247.721	890.004
	NL	11.010	119.245	487.468	1777.397

the present results are in good agreement with those of Refs. [6,10].

In Tables 2–10, the results of thermal buckling analysis for FG annular sector plate under both uniform temperature rise (U) and nonlinear temperature change across the thickness (NL), for nine possible boundary conditions, are presented. In these Tables, it is assumed that the initial temperature rise is equal to 5 °C in the metal-rich surface of the plate [10].

Tables 2–4 illustrate the critical buckling temperature for symmetric boundary conditions *SSSS*, *SSCC* and *SSFF*, respectively. It can be seen that the critical buckling temperature increases with decreasing the radius–thickness ratio b/h and decreases with increasing the power law index n. Also, the buckling temperature changes very slowly when the power law index n is greater than 2. Moreover, it increases rapidly with decreasing b/h for $b/h \leqslant 10$. By comparing the results of these Tables, it can be

Table 5
Thermal buckling temperature of SSCF functionally graded annular sector plate under uniform temperature rise (U) and nonlinear temperature change across the thickness (NL) for some values of n and $b/h(\beta = 60, b/a = 3)$.

n		$b/h = 50$	$b/h = 20$	$b/h = 10$	$b/h = 5$
0	U	29.065	177.867	678.458	2414.985
	NL	48.130	345.735	1346.916	4819.971
0.5	U	16.478	101.005	386.667	1387.604
	NL	30.275	253.229	1006.710	3646.840
1	U	13.515	82.907	317.908	1145.128
	NL	22.168	202.816	814.601	2968.118
2	U	11.981	73.484	281.673	1013.748
	NL	16.855	165.342	667.970	2435.417
5	U	12.348	75.537	287.876	1022.687
	NL	15.819	151.846	608.952	2190.789
20	U	12.141	74.101	281.015	987.334
	NL	14.342	138.779	554.333	1972.870

Table 6
Thermal buckling temperature of SSCS functionally graded annular sector plate under uniform temperature rise (U) and nonlinear temperature change across the thickness (NL) for some values of n and $b/h(\beta = 60, b/a = 3)$.

n		$b/h = 50$	$b/h = 20$	$b/h = 10$	$b/h = 5$
0	U	174.096	1046.822	3717.667	10573.946
	NL	338.192	2083.645	7425.334	21137.892
0.5	U	98.722	595.994	2140.317	6246.007
	NL	247.206	1558.843	5632.243	16461.661
1	U	80.979	489.758	1767.701	5220.474
	NL	197.798	1261.980	4588.876	13577.546
2	U	71.786	433.987	1564.625	4608.280
	NL	161.242	1035.702	3765.399	11113.685
5	U	73.961	444.278	1573.512	4448.006
	NL	148.453	945.639	3376.557	9564.516
20	U	72.695	434.178	1514.141	4136.780
	NL	135.955	861.939	3030.881	8298.055

Table 7
Thermal buckling temperature of SSFC functionally graded annular sector plate under uniform temperature rise (U) and nonlinear temperature change across the thickness (NL) for some values of n and $b/h(\beta = 60, b/a = 3)$.

n		$b/h = 50$	$b/h = 20$	$b/h = 10$	$b/h = 5$
0	U	191.888	1156.959	4113.265	11443.021
	NL	373.776	2303.918	8216.531	22876.042
0.5	U	108.802	658.530	2368.823	6782.925
	NL	273.794	1723.791	6234.964	17877.869
1	U	89.244	541.081	1956.630	5678.153
	NL	219.315	1395.591	5080.718	14769.031
2	U	79.114	479.478	1731.813	5010.517
	NL	178.934	1145.532	4169.040	12084.805
5	U	81.521	491.050	1740.785	4809.507
	NL	164.727	1046.326	3736.646	10342.722
20	U	80.135	480.042	1673.988	4451.660
	NL	150.897	954.050	3351.910	8930.444

Table 8
Thermal buckling temperature of SSFS functionally graded annular sector plate under uniform temperature rise (U) and nonlinear temperature change across the thickness (NL) for some values of n and $b/h(\beta = 60, b/a = 3)$.

n		$b/h = 50$	$b/h = 20$	$b/h = 10$	$b/h = 5$
0	U	130.621	797.962	2955.943	9135.503
	NL	251.242	1585.925	5901.886	18261.006
0.5	U	74.042	453.433	1693.015	5353.664
	NL	182.110	1182.814	4452.411	14107.963
1	U	60.725	372.285	1394.953	4457.620
	NL	145.072	956.162	3618.494	11591.593
2	U	53.834	329.955	1235.362	3938.312
	NL	117.900	784.539	2970.461	9496.185
5	U	55.496	338.821	1252.669	3850.012
	NL	108.704	718.621	2685.874	8277.207
20	U	54.574	332.022	1213.813	3616.08
	NL	99.563	656.774	2427.717	7252.321

Table 9
Thermal buckling temperature of SSSC functionally graded annular sector plate under uniform temperature rise (U) and nonlinear temperature change across the thickness (NL) for some values of n and $b/h(\beta = 60, b/a = 3)$.

n		$b/h = 50$	$b/h = 20$	$b/h = 10$	$b/h = 5$
0	U	228.678	1369.114	4766.860	12641.480
	NL	447.357	2728.228	9523.720	25272.961
0.5	U	129.682	779.976	2752.674	7529.671
	NL	328.870	2044.124	7247.433	19847.530
1	U	106.379	641.120	2276.494	6317.855
	NL	263.922	1656.024	5913.426	16434.381
2	U	94.302	568.077	2014.364	5572.066
	NL	215.602	1359.437	4851.203	13440.550
5	U	97.147	580.968	2016.065	5307.219
	NL	198.367	1239.895	4329.246	11414.155
20	U	95.474	567.228	1931.511	4882.664
	NL	181.704	1129.151	3869.105	9796.051

Table 10
Thermal buckling temperature of SSSF functionally graded annular sector plate under uniform temperature rise (U) and nonlinear temperature change across the thickness (NL) for some values of n and $b/h(\beta = 60, b/a = 3)$.

n		$b/h = 50$	$b/h = 20$	$b/h = 10$	$b/h = 5$
0	U	26.324	162.124	627.489	2288.811
	NL	42.649	314.248	1244.979	4567.621
0.5	U	14.922	91.998	357.017	1312.295
	NL	26.171	229.471	928.503	3448.201
1	U	12.238	75.488	293.301	1081.851
	NL	18.843	183.504	750.540	2803.389
2	U	10.849	66.914	259.916	957.959
	NL	14.122	149.479	615.444	2300.727
5	U	11.184	68.863	266.357	969.732
	NL	13.313	137.479	562.627	2076.791
20	U	10.999	67.622	260.587	938.638
	NL	12.049	125.768	513.308	1875.071

Table 11
Thermal buckling temperature of simply supported; SSSS functionally graded annular sector plate under uniform temperature rise for some values of n and $\beta(b/a = 3, b/h = 50)$.

n	$\beta = 30$	$\beta = 45$	$\beta = 60$	$\beta = 90$	$\beta = 120$	$\beta = 180$	$\beta = 210$	$\beta = 270$	$\beta = 360$
0	333.984	198.367	147.455	111.024	98.793	90.496	88.805	86.991	85.798
0.5	189.455	112.470	83.589	62.929	55.994	51.290	50.331	49.303	48.627
1	155.430	92.952	68.557	51.609	45.921	42.062	41.276	40.433	39.878
2	137.781	81.780	60.776	45.753	40.710	37.289	36.592	35.845	35.353
5	141.873	84.274	62.648	47.171	41.975	38.450	37.731	36.961	36.454
20	139.371	82.847	61.603	46.393	41.285	37.819	37.113	36.355	35.857

said that the *SSCC* plate has the maximum critical buckling temperature and the *SSFF* plate has the minimum critical buckling temperature.

In Tables 5–11 the results of thermal buckling analysis for non-symmetric boundary conditions are presented. It can be concluded that the critical buckling temperature increases by decreasing the radius–thickness ratio, b/h, and decreases with increasing the power law index n . For all of these cases, when the power law index n is greater than 2, the change of the critical buckling temperature is slight.

By comparing the buckling temperatures for two different types of loading, it can be concluded that the buckling temperature for nonlinear temperature change is greater than that of the uniform temperature rise.

To study the effects of sector angle on buckling temperature of FG annular sector plate, the critical buckling temperature under uniform temperature rise for *SSSS* boundary condition are presented in Table 11. This Table shows that the buckling temperature decreases by increasing the sector angle for all different sector angles.

In the case of uniform temperature rise, Fig. 2 shows the critical buckling temperature T_{cr} versus the aspect ratio b/a and power law index n for symmetric boundary conditions. The parameters are taken to be $\beta = 60, n = 1$ and $b/h = 20$. It can be seen form this figure that increasing the aspect ratio b/a, decreases the critical buckling temperature, T_{cr}, except for *SSFF* boundary condition.

In addition, for non-symmetric boundary conditions, Fig. 3 depicts the critical buckling temperature T_{cr} versus the aspect ratio b/a and power law index n. From this figure, it can be seen that by increasing the aspect ratio b/a, the critical buckling temperature, T_{cr}, decreases except for the plates with free inner circular edges. Also, the critical buckling temperature for *SSCF* and *SSSF* boundary conditions are close to each other and lower than that of other boundary conditions. Moreover, for large amounts of b/a, the boundary condition in inner circular edges does not affect the critical buckling load.

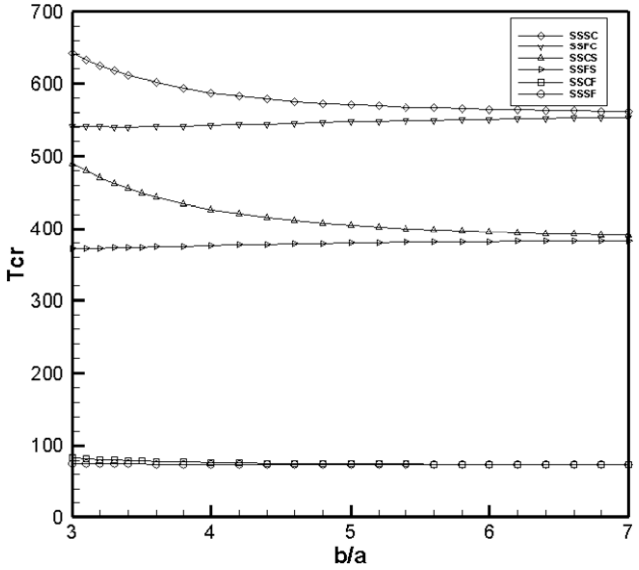

Fig. 3. Critical buckling temperature of FG plate under uniform temperature rise versus aspect ratio b/a for non-symmetric boundary conditions ($\beta = 60, n = 1$, $b/h = 20$).

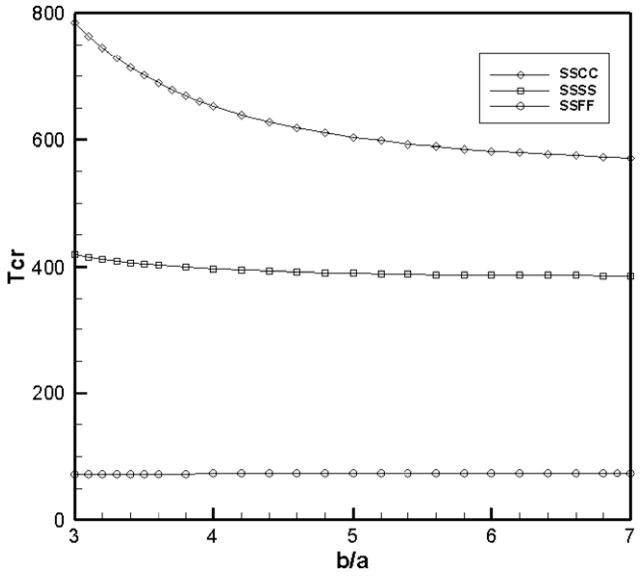

Fig. 2. Critical buckling temperature of FG plate under uniform temperature rise versus aspect ratio b/a for symmetric boundary conditions ($\beta = 60, n = 1$, $b/h = 20$).

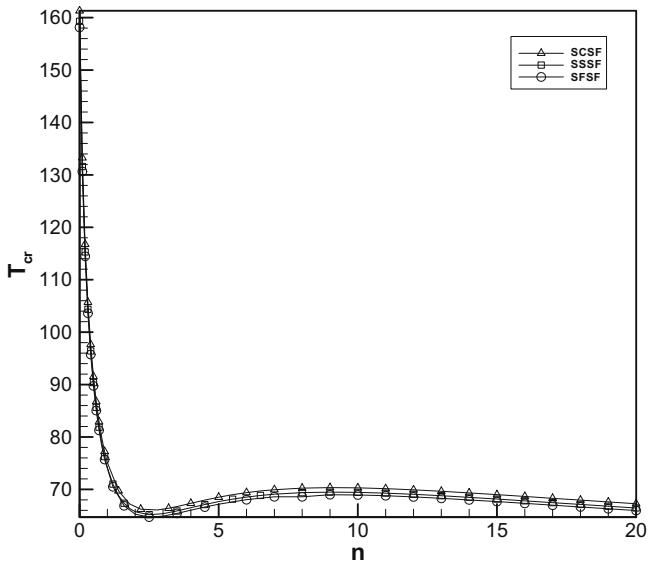

Fig. 4. Critical buckling temperature of FG plate under uniform temperature rise versus power law index n for boundary conditions containing free outer edge ($b/h = 20, b/a = 5, \beta = 60$).

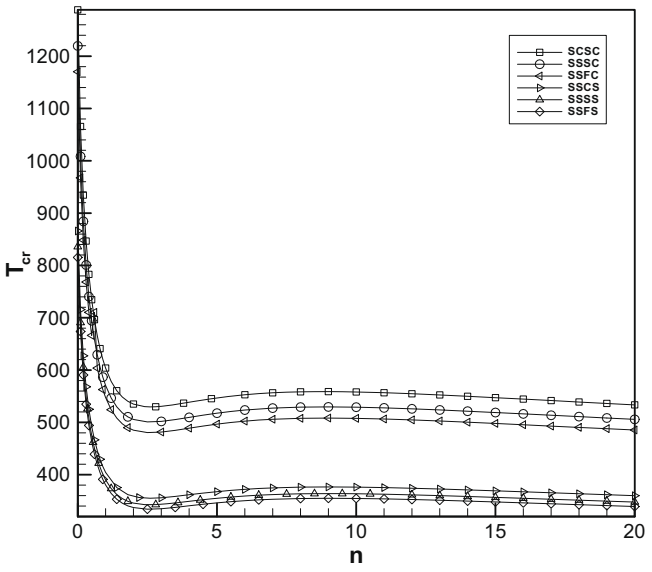

Fig. 5. Critical buckling temperature of FG plate under uniform temperature rise versus power law index n for various boundary conditions ($b/h = 20, b/a = 5, \beta = 60$).

Furthermore, Figs. 4 and 5 show the critical buckling temperature versus the power law index n for FG plates with free outer edge and other boundary conditions, respectively. It can be seen that by increasing n, the critical buckling temperature decreases for ($n \leqslant 2$) and increases for ($2 < n < 12$) and then decreases for ($n \geqslant 12$). This behavior can be also seen from Tables 2–11.

7. Conclusions

In this paper, the equilibrium and stability equations for FG annular sector plates under both uniform temperature rise and nonlinear temperature change across the thickness have been derived based on the first order shear deformation plate theory. It is assumed that the annular sector plate has simply supported boundary conditions in radial edges and arbitrary boundary conditions along the circular edges. The coupled stability equations have been converted to two decoupled partial differential equations and two algebraic equations. The critical buckling temperature has been obtained for nine different boundary conditions along the circular edges. The following conclusions can be remarked:

1. The critical buckling temperatures for functionally graded plates are generally lower than the corresponding values for homogeneous ceramic plates.
2. The critical buckling temperature of a FG annular sector plate increases when the radius–thickness ratio b/h and/or the power law index $n$decreases.
3. The critical buckling temperature of FG annular sector plates decreases by increasing the aspect ratio b/a except for the plates with free inner circular edge.
4. The critical buckling temperature of FG annular sector plates decreases by increasing the sector angle.
5. For FG plates under nonlinear temperature change across the thickness, the critical buckling temperature is greater than that of uniform temperature distribution.
6. For uniform temperature rise when the power law index n is greater than 2, the critical buckling temperature changes very slowly by changing n.
7. For FG plates under uniform temperature rise, by increasing the power law index n, the critical buckling temperature decreases for ($n \leqslant 2$) and increases for ($2 < n < 12$) and then decreases for ($n \geqslant 12$).
8. For the plates with free outer radius, the critical buckling temperatures are close to each other in all aspect ratios.

Acknowledgement

The authors wish to thank the reviewers for their precious comments and suggestions.

References

[1] Koizumi M. FGM activities in Japan. Composites Part B 1997;28(1–2):1–4.
[2] Birman V, Byrd LW. Modeling and analysis of functionally graded materials and structures. ASME J Appl Mech 2007;60:195–216.
[3] Fukui Y. Fundamental investigation of functionally gradient material manufacturing system using centrifugal force. Int J Jpn Soc Mech Eng 1991;4(1):144–8.
[4] Ventsel E, Krauthammer T. Thin plates and shells theory, analysis and applications. New York (USA): Marker Dekker Inc.; 2001.
[5] Javaheri R, Eslami MR. Thermal buckling of functionally graded plates. AIAA J 2002;40(1):162–9.
[6] Javaheri R, Eslami MR. Thermal buckling of functionally graded plates based on higher order theory. J Therm Stress 2002;25:603–25.
[7] Najafizadeh MM, Eslami MR. Thermo-elastic stability of orthotropic circular plates. J Therm Stress 2002;25(10):985–1005.
[8] Najafizadeh MM, Eslami MR. First order theory based thermo elastic stability of functionally graded material circular plates. AIAA J 2002;40: 1444–50.
[9] Najafzadeh MM, Heydari HR. Thermal buckling of functionally graded circular plates based on higher order shear deformation plate theory. Eur J Mech A/ Solids 2004;23:1085–100.
[10] Lanhe W. Thermal buckling of a simply supported moderately thick rectangular FG plate. Compos Struct 2004;64:211–8.
[11] Yang J, Liew KM, Kitipornchai S. Second-order statistics of the elastic buckling of functionally graded rectangular plates. Compos Sci Technol 2005;65:1165–75.
[12] Ganapathi M, Prakash T. Thermal buckling of simply supported functionally graded skew plates. Compos Struct 2006;74:247–50.
[13] Morimoto T, Tanigawa Y, Kawamura R. Thermal buckling of functionally graded rectangular plates subjected to partial heating. Int J Mech Sci 2006;48:926–37.
[14] Abrate S. Free vibration, buckling and static deflections of functionally graded plates. Compos Sci Technol 2006;66:2383–94.
[15] Samsam Shariat BA, Eslami MR. Thermal buckling of imperfect functionally graded plates. Int J Solids Struct 2006;43:4082–96.
[16] Samsam Shariat BA, Eslami MR. Buckling of thick functionally graded plates under mechanical and thermal loads. Compos Struct 2007;78:433–9.
[17] Saidi AR, Rasouli A, Sahraee S. Axisymmetric bending and buckling analysis of thick functionally graded circular plates using unconstrained third-order shear deformation plate theory. Compos Struct 2009;89:110–9.
[18] Sahraee S, Saidi AR. Axisymmetric bending analysis of thick functionally graded circular plates using Fourth order shear deformation theory. Eur J Mech A/Solids 2009;28:974–84.
[19] Jomehzadeh E, Saidi AR, Atashipour SR. An analytical approach for stress analysis of functionally graded annular sector plates. J Mater Des 2009;30:3679–85.
[20] Zhao X, Lee YY, Liew KM. Mechanical and thermal buckling analysis of functionally graded plates. Compos Struct 2009;90:161–71.
[21] Matsunaga H. Thermal buckling of functionally graded plates according to a 2D higher-order deformation theory. Compos Struct 2009;90:76–86.
[22] Reddy JN. Energy principles and variational methods in applied mechanics. 2nd ed. New York: John Wiley and Sons Inc.; 2002 [chapter 5].
[23] Reddy JN. Theory and analysis of elastic plates. Philadelphia: Taylor & Francis; 1999.
[24] Brush DO, Almroth BO. Buckling of bars, plates and shells. New York: McGraw–Hill; 1975 [chapter 3].
[25] Wang CM, Reddy JN, Lee KH. Shear deformation beams and plates relationships with classical solutions. Elsevier Science Ltd.; 2000.
[26] Meyers CA, Hyer MW. Thermal buckling and post buckling of symmetrically laminated composite plates. J Therm Stress 1991;l(14):519–40.
[27] Watson GN. Theory of bessel functions. 2nd ed. Cambridge: Cambridge University Press; 1994.
[28] Nosier A, Reddy JN. On vibration and buckling of symmetric laminated plates according to shear deformation theories. Acta Mech 1992;94:145–69.